

Fracture Behavior and Mechanical Properties of WC-Co Subjected to Thermal Shock

Dong-Bin Han and John J. Mecholsky, Jr.*

Department of Materials Science and Engineering
Pennsylvania State University, University Park, PA 16802, U.S.A.

*Presently at University of Florida

(Received December 7, 1989)

WC-Co 의 열충격 후 파괴 현상과 기계적 성질

한동빈 · John J. Mecholsky Jr.*

Department of Materials Science and Engineering
Pennsylvania State University, University Park, PA 16801, U.S.A.

* 현재 University of Florida 재료공학과 교수

(1989년 12월 7일 접수)

ABSTRACT

WC-Co composites are widely used as cutting or drilling tools because of their high hardness, strength, and fracture toughness. The working temperature is, however, generally in the range of 300-700°C so thermal shock fracture of WC-Co can occur. In this study, the strength, fracture toughness and fracture surface of 16wt% Co bonded tungsten carbide composites before and after thermal shock were observed.

요 약

WC-Co 복합 재료는 강도, 경도, 그리고 파괴인성이 높아 절삭 공구 등에 널리 이용되고 있다. 그러나 작업 온도가 300-700°C에 이르고 있어 급가열, 급냉에 따른 열충격 파괴가 쉽게 일어난다. 이 연구에서는 열충격후 파괴강도와 파괴인성의 변화를 알아 보았다. 또한, 열충격이 시편의 미세 구조에 어떤 변화를 미치는지 파괴단면을 관찰하였다.

INTRODUCTION

The ability of WC-Co composites to withstand high temperature is one of the major concerns determining their application. However, their characteristic brittle nature and generally low thermal conductivity leaves them susceptible to thermal shock damage and fracture. High tensile stresses at the surface on rapid

cooling may cause considerable cracking damage and possible catastrophic failure, if thermal stress exceeds the strength of the material¹⁻⁴⁾.

Kingery⁵⁾ has examined numerous factors affecting thermal shock. It was concluded that materials are desired with high values of strength, thermal conductivity and thermal diffusivity combined with low thermal expansion coefficient and elastic modulus.

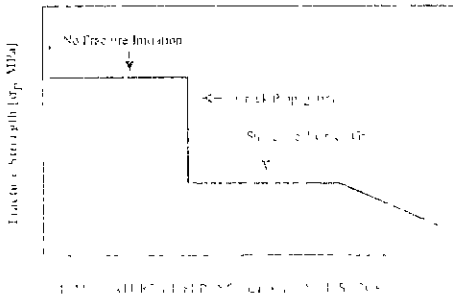


Fig.1. Proposed strength behavior of a brittle material subjected to thermal shock.

Experimental evidence supporting these parameters has been shown by many investigators, including Coble and Kingery⁶⁾, and Hasselman and Crandall⁷⁾.

Thermal stress theory predicts distinct regions of behavior for a material based on thermal shock (Fig. 1)⁸⁻¹⁰⁾. In the region of least thermal shock, flaws present within the material are subcritical with respect to the thermal shock. Therefore, no significant damage is initiated and no change in the strength is observed for materials subjected to this degree of thermal shock. The next region occurs upon reaching a critical degree of severity of thermal shock. Here, cracks grow to a new length and an instantaneous decrease in strength results. The third region shows little or no further loss in strength because the flaws are subcritical in length require a higher degree of thermal shock to extend the cracks. In the most severe thermal shock region, another critical degree of extremely severe thermal shocking is reached and cracks are again unstable with respect to the temperature change. The cracks will propagate even more extensively, resulting in a gradual decrease in strength with increased severity thermal shock. The severity of the transition depends on the flaw distribution in the material. The larger the standard deviation of the strength, the wider the transition in temperature.

This type of strength behavior has been observed by several workers for Al₂O₃¹⁰⁻¹²⁾, ZnO¹³⁾ and TiC¹⁴⁾. However, it has been reported¹⁵⁾ that some materials

do not follow the generally accepted Hasselman theory⁹⁾ for thermal shock in brittle materials and residual strength fell gradually at temperatures lower than the expected critical quenching temperature. Mai and Atkins¹⁴⁾, have applied Hasselman's theory of thermal shock to examine the retained strength of carbide tools after heat treatment and they reported that the retained strength was low because the pre-existing small internal flaws in the carbides grew during the critical shock.

In general, tests for thermal shock^{11,15)} are essentially of two types: determination of the minimum shock to nucleate cracking (thermal stress resistance parameter) and determination of the amount of damage sustained by a fixed shock or series of shock (thermal shock damage resistance parameter). Mai and Atkins¹⁴⁾ also suggested that carbide tools could be compared according to both resistance to crack initiation and resistance to crack propagation.

The critical quenching temperature difference (ΔT_c) could be approximately estimated from equation (1)^{10,11)}

$$\Delta T_c = \frac{3.25}{ah} (1 - \nu) \left(\frac{k \sigma_f}{E \alpha} \right) \dots \dots \dots (1)$$

where a is the half plate thickness, h is the heat transfer coefficient, ν is Poissons ratio, k is the thermal conductivity, α is the thermal expansion coefficient, σ_f is the flexural strength at room temperature and E is elastic modulus

The present paper reports the results of an experimental investigation on the thermal shock resistance and fracture strength behavior of 16wt% Co bonded tungsten carbides.

EXPERIMENTAL PROCEDURES

The sintered 16wt% cobalt bonded tungsten carbide composites* were used. Table 1 summarizes the properties of the material used in this study 5 specimens were heated at a rate of 20°C/min up to

* DBS Co Houston, TX

Table 1. The Properties of WC-16wt% Co

ν^*	k^* cal/s °Ccm	α^* °C ⁻¹	h cal/s °Ccm ²	E^* GPa	σ_f MPa	K_{Ic} MPa√m
0.22	0.12	6×10^{-6}	1.0	560	1950	24.1

* DBS Co Data

400, 600, 800 and 1000°C, held for 15 minutes and quenched in a water bath at 20°C. Each specimen was then broken using 3-point flexure for strength measurements. The oxidation layer was analyzed using X-ray diffraction.

Fracture toughness was measured using an indentation technique before and after water-quenching. To remove grinding damage on the surface before indentation, three sequential polishing steps were required: 3 minutes on 15μm, 10 minutes on 6μm, and 10 minutes on 1μm diamond grit wheel using an automatic polisher. After polishing, all indentations were made at 2000N with a diamond Vickers indenter using screw driven tensile testing machine**. The loading speed was 0.0005mm/sec, held for 15 seconds and released at the same speed as that of loading. Crack sizes were determined by optical microscopy. Fracture toughness, K_{Ic} , was evaluated using an indentation technique¹⁶⁾(Eq. 2)

$$K_{Ic} = 0.016 \sqrt{[E/H]Pc^{-3/2}} \dots \dots \dots (2)$$

In above equation, P is the indentation load, c the crack length, H the hardness, and E the elastic modulus.

RESULTS AND DISCUSSION

The specimens after thermal shock tests are shown in Fig.2A. The darker color of the specimen at 600°C indicates the initiation of the oxidation process. The oxidation layer can be easily seen by the unaided eye for specimen from 800°C and above. The average thickness of the oxidation layer was 190μm at 800°C

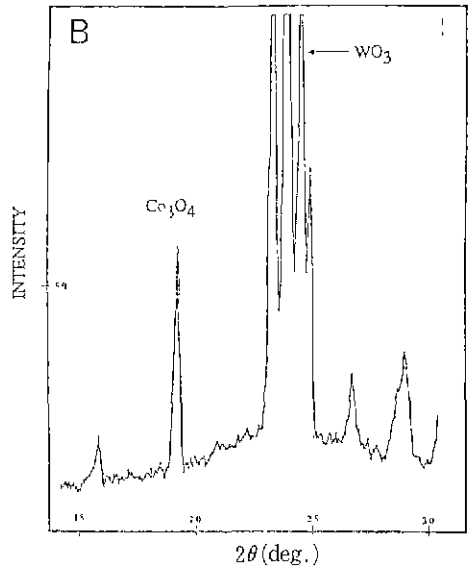
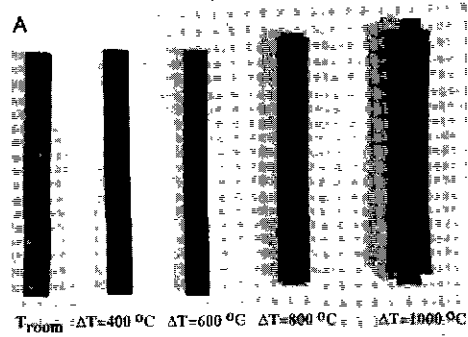


Fig. 2. Appearance change of thermally shocked WC-16wt% Co due to oxidation (A) and X-ray diffraction analysis indicates WO_3 and Co_3O_4 are the major oxidation products (B).

and 340μm at 1000°C, respectively. In Fig 2B, X-ray diffraction analysis indicates tungsten mainly oxidizes, with minor oxidation of the cobalt phase.

Fig 3 shows the strength degradation behavior of thermally shocked WC-16wt% Co. The strength was calculated based on the original dimension before thermal shock test. It is better to exhibit the thermal shock property using relation of load-carrying capacity to quenching temperature difference for oxidizable materials because of dimension change. However, either strength or load-carrying capacity remains essentially constant for temperature differenc-

** Instron Eng Corp., Canton, MA

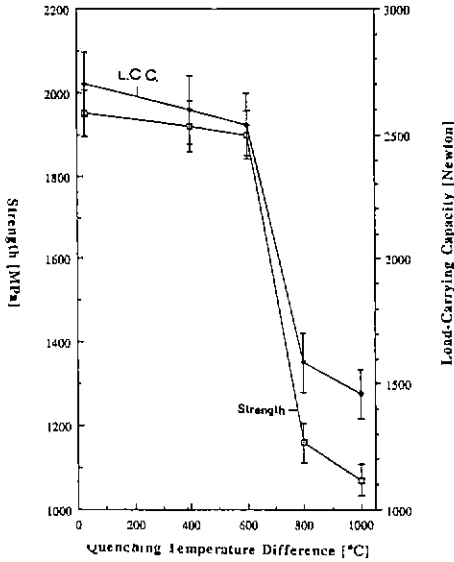


Fig.3. Relation of strength and load-carrying capacity of WC-Co composite to quenching temperature difference.

es of up to 600°C and then decreases with further increase in thermal shock temperature difference. This behavior agrees with the prediction of

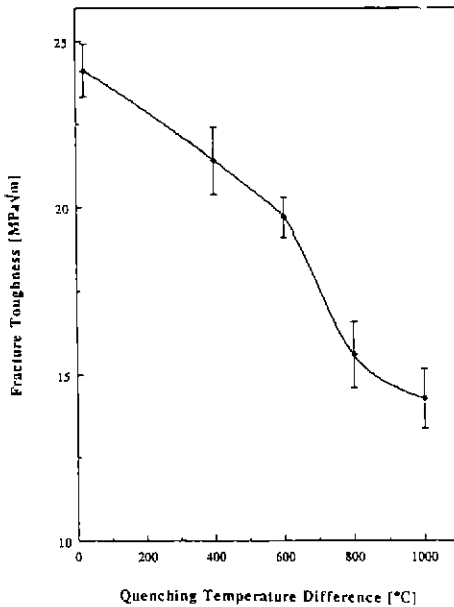


Fig.4. Fracture toughness change as a function of thermal shock severity.

Hasselmann's theory⁹⁾. Mai¹⁰⁾ reports that strength loss is a result of subcritical crack growth caused by plastic deformation within the metal phase or surface residual stress during thermal shock

Substitution of values in Table 1 into Eq (1) results in $\Delta T_c=1100^\circ\text{C}$ for 16wt% Co bonded WC when $h=1$ cgs unit. The crack initiation parameter $[k\sigma_f/E\alpha]$ caused by thermal shock yields about 163.5 cal/cm/sec. The thermal-shock-damage parameters $[K_c/\sigma_f]^2$ are $1134\mu\text{m}$, $1840\mu\text{m}$ and $1850\mu\text{m}$ at $\Delta T=600^\circ\text{C}$, 800°C , and 1000°C , respectively. The observation from strength measurements and thermal shock damage parameter indicates that ΔT_c is approximately 700°C for WC-16wt% Co composites. The retained strength in fact falls off well before the predicted critical temperature. The reason for the departure from Hasselmann's model seems to be bound upon

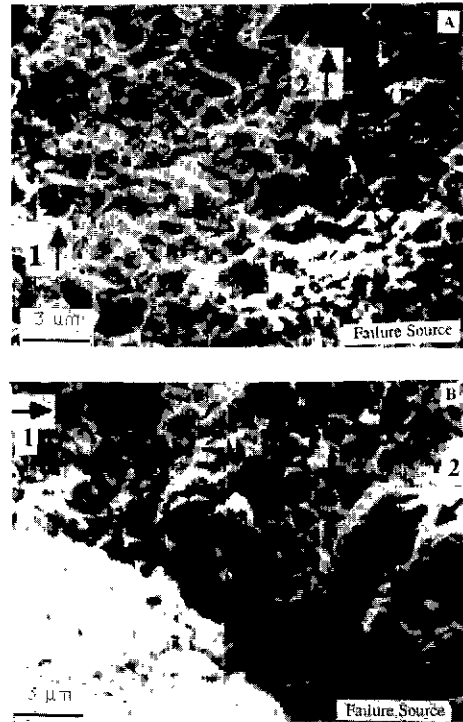


Fig.5. SEM micrographs taken above indentation crack (A) and oxidation flaw (B) show that WC particles mainly fracture transgranularly after thermal shock.

reduction in strength (Fig.3) and fracture toughness (Fig.4) of WC-Co with increasing quenching temperature difference.

It is reasonable to assume that some fracture micromechanisms must account for the strength degradation behavior between 600°C and 800°C. Plausible mechanisms include subcritical crack extension due to thermal stress, microcracking of WC particles (Fig.5), partial oxidation of WC particles/cobalt phase (Fig.2B) or water-assisted stress corrosion during quenching. Previous research¹⁷⁾ on failure analysis of WC-Co shows that WC grains less than 4-5µm mainly fracture intergranularly at ambient temperature. However, photos in Fig.5 show that fracture paths are mainly transgranular for both small grains (arrow 1) and large grains (arrow 2).

The SEM micrographs in Fig.6 show fracture surfaces of unindented specimens for each ΔT. The roughness on the fracture surface becomes less severe

with increasing ΔT, indicating a decrease in the strength of sample. It can be seen that the specimens at 400[6-A] and 600°C[6-B] failed due to microstructural processing defects. It is most likely that the oxidation process weakens the surface and creates surface flaws [6-C & 6-D]. Fig.7A shows the microstructure above failure-initiating flaw corresponding circle region in Fig.6C. The X-ray analysis of the dark particle (arrow) indicates that tungsten oxidizes by oxygen diffusion during heat-treatment, thereby reducing its fracture resistance.

SUMMARY

The prediction by Hasselman's theory for critical temperature difference, ΔT_c, should be reconsidered even though behavior of strength degradation vs ΔT approximately follows the theory which does not account for the reduction in strength after thermal

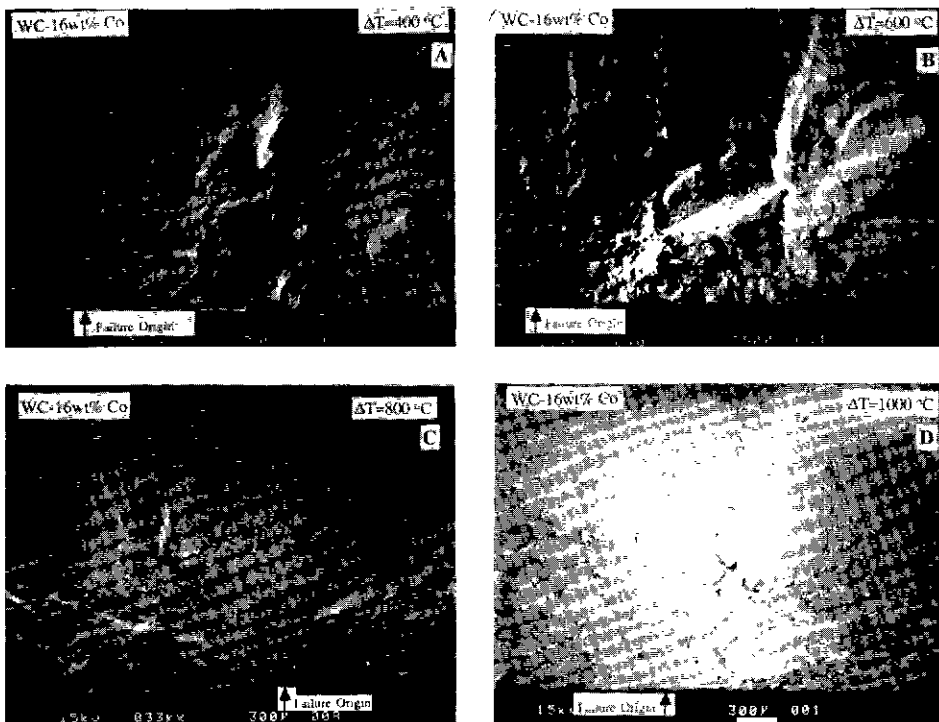


Fig. 6. SEM micrographs showing fracture surfaces of specimens after thermal shock at different quenching differences.

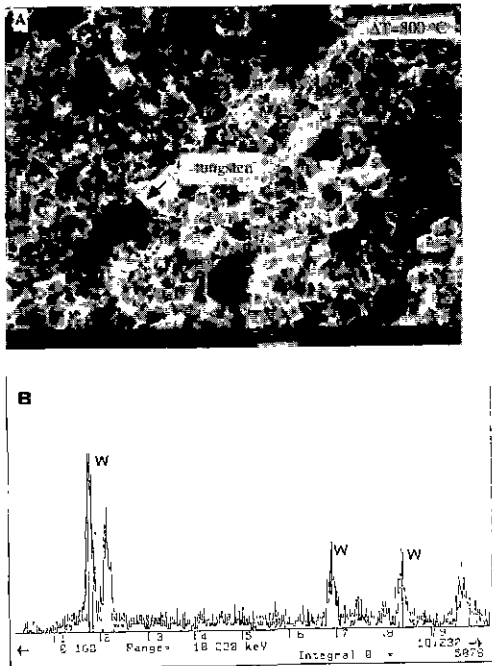


Fig.7. SEM (A) and X-ray (B) analysis around failure-initiating flaw of thermally shocked specimen ($\Delta T=800^{\circ}\text{C}$).

shock. It is usually assumed that the fracture toughness remains almost constant in thermal shock test. This study, however, reveals that the fracture toughness decreases with increasing quenching temperature.

Fracture surface analyses show that an oxidation layer creates surface defects which act as the failure initiating flaws. The thermal shock stress seems to change failure pattern, i.e., more transgranular fractures even for the small grains.

REFERENCES

1. C.W. Merten, "Response of a WC-Co Alloy to Thermal Shock", *Science of Hard Materials*, R. K. Viswanadham, D.J. Rowcliffe, and J. Gurland(ed), Plenum Press, New York, 757-774 (1983).
2. A.A. Betser and J. Gurland, "Some Effects of Temperature and Heat Treatment on the Strength of Sintered WC-Co Alloys", ASME 66-MD-17 (1966).
3. G.S. Kreimer, "Strength of Hard Alloys", Consultants Bureau, New York (1968).
4. J.A. Coppola, "Investigation of the Fracture Surface Energy, Fracture Strength and Thermal Shock Behavior of Polycrystalline Materials", Ph. D. Thesis, The Pennsylvania State University, (1971).
5. W.D. Kingery, "Factors Affecting Thermal Shock Resistance of Ceramic Materials", *J. Am. Ceram. Soc.*, **38** (1) 3-15 (1955)
6. R.L. Coble and W.D. Kingery, "Effect of Porosity on Thermal Stress Fracture", *ibid.*, **38** (1) 33-38 (1958).
7. D.P.H. Hasselman and W.B. Crandall, "Thermal Shock Analysis of Spherical Shapes, II", *ibid.*, **46** (9) 434-437 (1963).
8. D.P.H. Hasselman, "Elastic Energy at Fracture and Surface Energy as Design Criteria for Thermal Shock", *ibid.*, **46** (11), 535-540 (1963).
9. D.P.H. Hasselman, "Unified Theory of Thermal Shock Fracture Initiation and Crack Propagation in Brittle Ceramics", *ibid.*, **52** (11) 600-604 (1969).
10. D.P.H. Hasselman, "Strength Behavior of Polycrystalline Alumina Subjected to Thermal Shock", *J. Am. Ceram. Soc.*, **53** (9), 490-495 (1970).
11. R.W. Davidge and G. Tappin, "Thermal Shock and Fracture in Ceramics", *Trans. British Ceram. Soc.*, **66** (8) 405-422 (1967).
12. J.H. Ainsworth and R.E. Moore, "Fracture Behavior of Thermally Shocked Aluminium Oxide", *J. Am. Ceram. Soc.*, **52** (11) 628-629 (1969).
13. T.K. Gupta, "Strength Behavior of Thermally Shocked ZnO", *ibid.*, **55** (8) 429 (1972).
14. Y.W. Mai and A.G. Atkins, "Fracture Toughness and Thermal Shock of Tool and Turbine Ceramics", *J. Mater. Sci.*, **10** (11)

- 1904-1919 (1975).
15. Y W. Mai, "Thermal-Shock Resistance and Fracture-Strength Behavior of Two Tool Carbides", *J Am. Ceram. Soc.*, **59** (12) 491-494 (1976).
16. G.R. Anstis, P. Chantikul, B.R. Lawn, and D. B. Marshall, "A Critical Evaluation of Indentation Techniques for Measuring Fracture Toughness- I, Direct Crack Measurements", *ibid.*, **64** (9) 533-538 (1981).
17. Dong-Bin Han and J.J. Mecholsky, "Fracture Analysis and Failure Behavior of WC-Co Composites by Fracture Surface Analysis", *J. Kor. Ceram. Soc.*, **26** (5) 645-654 (1989).